

## ORIGINAL ARTICLE

# Reticulocalbin3: A Ca<sup>2+</sup> homeostasis regulator that promotes esophageal squamous cell carcinoma progression and cisplatin resistance

Rui Cai<sup>1,2,3</sup> | Ping Wang<sup>1,2,3</sup> | Xin Zhao<sup>1,2,3</sup> | Xiansheng Lu<sup>1,2,3</sup> | Ruxia Deng<sup>1,2,3</sup> | Xiaoyu Wang<sup>1,2,3</sup> | Chang Hong<sup>1,2,3</sup> | Jie Lin<sup>1,2,3</sup> 

<sup>1</sup>Department of Pathology, Nanfang Hospital, Southern Medical University, Guangzhou, China

<sup>2</sup>Department of Pathology, School of Basic Medical Sciences, Southern Medical University, Guangzhou, China

<sup>3</sup>Guangdong Province Key Laboratory of Molecular Tumor Pathology, Guangzhou, China

## Correspondence

Jie Lin, Department of Pathology, Nanfang Hospital, Southern Medical University, Guangzhou 510515, China.  
Email: [jielin\\_gz@126.com](mailto:jielin_gz@126.com)

## Funding information

Guangzhou Science and Technology Project, Grant/Award Number: 202102080076; National Natural Science Foundation of China, Grant/Award Number: 81672441 and 82173298; Natural Science Foundation of Guangdong Province, Grant/Award Number: 2016A030313580, 2017A030313607 and 2022A1515012390

## Abstract

Esophageal squamous cell carcinoma (ESCC) is one of the most prevalent cancers worldwide. There is a critical need to identify new mechanisms that contribute to ESCC progression. Reticulocalbin3 (RCN3) is mainly located in the endoplasmic reticulum and Ca<sup>2+</sup>-binding protein containing EF-hands. The function of RCN3 in tumor progression has not been clarified. We observed that the expression level of RCN3 was higher in ESCC tissues than in paired normal tissues. Overexpression of RCN3 was positively associated with tumor size, lymph node metastasis, TNM stage, lymphatic vessel infiltration, and poor outcome in patients with ESCC. Increased malignant phenotypes were observed in RCN3 overexpressing ESCC cells, whereas the opposite effects were achieved in RCN3-silenced cells. Reticulocalbin3 promoted the expression of MMP-2 and MMP-9 by regulating the inositol 1,4,5-trisphosphate receptor 1 (IP3R1)-Ca<sup>2+</sup>-calcium/calmodulin-dependent protein kinase II-c-Jun signaling pathway. Reticulocalbin3 induced cisplatin resistance by regulating IP3R1/Ca<sup>2+</sup> to maintain intracellular Ca<sup>2+</sup> homeostasis and reduced reactive oxygen species in ESCC cells. Finally, the expression of RCN3 was regulated by hypoxia inducible factor-1 $\alpha$ . Collectively, these data strongly support that RCN3 regulates Ca<sup>2+</sup> homeostasis by targeting IP3R1 to promote the progression and platinum resistance of ESCC. Our studies suggest that RCN3 could serve as predictive factor of poor prognosis and potential therapeutic target for ESCC patients.

## KEYWORDS

Ca<sup>2+</sup> homeostasis, esophageal squamous cell carcinoma, metastasis, platinum resistance, RCN3

**Abbreviations:** ABCG2, ATP binding cassette subfamily G member 2; CaMK, calcium/calmodulin-dependent protein kinase; Co-IP, co-immunoprecipitation; DDP, cisplatin; EC, esophageal carcinoma; ER, endoplasmic reticulum; ESCC, esophageal squamous cell carcinoma; GO, Gene Ontology; HIF-1 $\alpha$ , hypoxia inducible factor-1 $\alpha$ ; IHC, immunohistochemistry; IP, immunoprecipitation; IP3R1, inositol 1,4,5-trisphosphate receptor 1; MDR1, multidrug resistance gene 1; NSCLC, non-small-cell lung cancer; qPCR, quantitative PCR; RCN3, reticulocalbin 3; ROS, reactive oxygen species; RYR1, ryanodine receptor 1; TEM, transmission electron microscope; TMT, tandem mass tag; TRG, tumor regression grading; WB, western blot.

Rui Cai and Ping Wang contributed equally to this work.

This is an open access article under the terms of the [Creative Commons Attribution-NonCommercial-NoDerivs](https://creativecommons.org/licenses/by-nc-nd/4.0/) License, which permits use and distribution in any medium, provided the original work is properly cited, the use is non-commercial and no modifications or adaptations are made.

© 2022 The Authors. *Cancer Science* published by John Wiley & Sons Australia, Ltd on behalf of Japanese Cancer Association.

## 1 | INTRODUCTION

Esophageal carcinoma is one of the most prevalent malignant tumors in the world. Its mortality rate ranks in the top 10 among all malignant tumors according to 2021 Cancer Statistics.<sup>1</sup> The incidence and mortality of esophageal cancer in China are both higher than the global average.<sup>2</sup> Esophageal squamous cell carcinoma comprises over 90% of all EC cases in China. The 5-year survival rate of EC patients is reportedly only approximately 20%.<sup>3</sup> Poor prognoses of ESCC are attributed to early metastasis and platinum-based chemotherapy resistance.<sup>4,5</sup> Therefore, looking for more sensitive and specific molecular targets of ESCC is of great importance for the cure of this malignant disease.

Reticulocalbins are Ca<sup>2+</sup>-binding protein containing EF-hands, have chaperone activity, and participate in the protein secretion process.<sup>6</sup> Accumulating evidence suggests that RCN family members might play a role in tumorigenesis and tumor progression. It has been reported that RCN1 and RCN2 are overexpressed in a variety of malignant tumors, including liver cancer,<sup>7</sup> NSCLC,<sup>8</sup> colorectal cancer,<sup>9</sup> glioblastoma,<sup>10</sup> renal cell carcinoma,<sup>11</sup> and prostate cancer.<sup>12</sup> These results also indicate that RCNs could play oncogenic roles in human malignancies and facilitate tumor cell metastasis.

As a member of the RCN family, RCN3 has been found to regulate ovarian follicle development,<sup>13</sup> participate in perinatal lung maturation,<sup>14</sup> and regulate fibrillogenesis.<sup>15,16</sup> There are fewer studies on RCN3 in tumors. Only studies on the expression of RCN3 in tumors has been reported. It is overexpressed in melanoma<sup>17</sup> and colorectal cancer,<sup>18</sup> but is expressed at low levels in osteosarcoma<sup>19</sup> and NSCLC.<sup>20</sup> The precise function of RCN3 in carcinogenesis deserves to be further investigated.

In a recent study, we found that RCN3 was upregulated in ESCC by comparing tissue protein expression in ESCC with adjacent tissues by TMT-based quantitative proteomics.<sup>21</sup> However, the function of RCN3 in ESCC progression has not been clarified. In this study, we evaluated the clinical role of RCN3 in ESCC. In particular, we investigated the effects of aberrant RCN3 expression on the cellular biological behavior of ESCC cells *in vitro* as well as *in vivo*. We also examined the role of RCN3 in relation to cisplatin resistance in ESCC cells. Finally, we found that RCN3 regulated Ca<sup>2+</sup> homeostasis by targeting IP3R1.

## 2 | MATERIALS AND METHODS

### 2.1 | Tissue samples

A total of 196 patients diagnosed with ESCC at Nanfang Hospital from 2017 to 2020 were enrolled in this study. None of 161 patients had received radiotherapy or chemotherapy before surgery. Both ESCC tumor tissues and adjacent tissues were collected. Thirty-five patients had received platinum-based neoadjuvant chemotherapy before surgery. Pretreatment biopsies and postoperative tissues were collected. Written informed consent was provided by all

patients. The use of human materials was approved by the Medical Ethical Committee of Nanfang Hospital. Pathological TNM staging was assessed according to the American Joint Committee on Cancer. Chemotherapy reactivity were defined by TRG.

### 2.2 | Cell culture

The cell lines TE-1, ECA109, KYSE150, and KYSE510 were authenticated by DNA short tandem repeat profiling before cells were received. The cell lines were grown in high glucose DMEM with 10% FBS (both from Gibco), augmented with 1% penicillin and streptomycin. Cells were maintained in an atmosphere of 5% CO<sub>2</sub> at 37°C.

### 2.3 | Establishment of DDP-resistant cell line

The resistant cell line was established *in vitro* by intermittent exposure to different concentrations of DDP in stepwise increments of time, starting with a concentration of 0.5 µg/ml. The drug concentration was increased to 0.5 µg/ml until the concentration was 20 µg/ml. Survival rates of different concentrations were tested by CCK-8 assay. The resistance index (RI) was calculated using the formula: RI = resistance cell IC<sub>50</sub>/normal cell IC<sub>50</sub>.

### 2.4 | Immunohistochemistry and immunofluorescence

The expression of protein in ESCC tissues was detected using an immunoperoxidase method. The slides were incubated in primary Ab (RCN3, Abcam, ab204178, 1:200; HIF-1α, Abcam, ab16066, 1:200), followed by treatment with secondary Ab, and a 3,3'-diaminobenzidine staining kit. The IHC intensity for each tissue slide was evaluated independently by two experienced pathologists who were blinded to patients' clinical data.

The total immunostaining score was calculated as the sum of the percentage positivity of stained tumor cells and the staining intensity. The positive percentage was scored from 0 to 4, as follows: 0, <5%; 1, 5%–25%; 2, 26%–50%; 3, >51%–75%; and 4, >75%. The staining intensity was scored from 0 to 3: 0, no staining; 1, weakly stained; 2, moderately stained; and 3, strongly stained. Then the whole score of protein expression was calculated with the value of the positive percentage score × staining intensity score, ranging from 0 to 12. The final expression level of RCN3 was defined as “low” (0–6) or “high” (7–12), and the final expression level of HIF-1α was defined as “low” (0–3) or “high” (4–12).

Cells were fixed with 4% paraformaldehyde and incubated in primary Abs (RCN3, Abcam, ab204178, 1:200; IP3R1, Santa Cruz Biotechnology, sc-271197, 1:100). The cells were washed with PBS three times, followed by treatment with CoraLite488 and CoraLite594 labeled IgG for 1 h. After washing the cells four times, cells were stained with DAPI.

## 2.5 | Real-time qPCR assays

Total RNA was isolated from cells using AG RNAex Pro Reagent AG21102 (Accurate Biotechnology (Human) Co., Ltd). RNA was reversely transcribed into cDNA by Evo M-MLV RT Premix for qPCR AG11706 (Accurate Biotechnology (Human) Co., Ltd). The information regarding primer sequences used in this study is summarized in Table S1.

## 2.6 | Western blot analysis

The proteins were separated by 10% SDS-PAGE and transferred to PVDF membranes (Millipore). The membranes were blocked in 5% skim milk for 2 h at room temperature then incubated with primary Abs overnight at 4°C: GAPDH (Proteintech, 10494-1-AP),  $\beta$ -tubulin (Proteintech, 10094-1-AP), RCN3 (Abcam, ab204178),

HIF-1 $\alpha$  (Proteintech, 20960-1-AP), IP3R1 (Santa Cruz Biotechnology, sc-271197), CaMKII (GeneTex, GTX52377), p-CaMKII (Santa Cruz Biotechnology, sc-32289), c-Jun (Santa Cruz Biotechnology, sc-166540), p-c-Jun (Santa Cruz Biotechnology), MMP2 (Proteintech, 66366-1-Ig), and MMP9 (Proteintech, 10375-2-AP). The PVDF membranes were washed three times for 15 min with PBST and incubated with HRP-conjugated secondary Ab for 90 min at room temperature. The PVDF membranes were washed three times for 15 min with PBST and visualized using ECL (Thermo Fisher Scientific).

## 2.7 | Transwell invasion assay

Transwell chambers were used to investigate cell invasion. After digestion and centrifugation, the cells were resuspended in FBS-free DMEM. Matrigel was added to the polycarbonate membrane. Cell suspension (100  $\mu$ l) at the density of  $3 \times 10^4$  cells/ml was placed

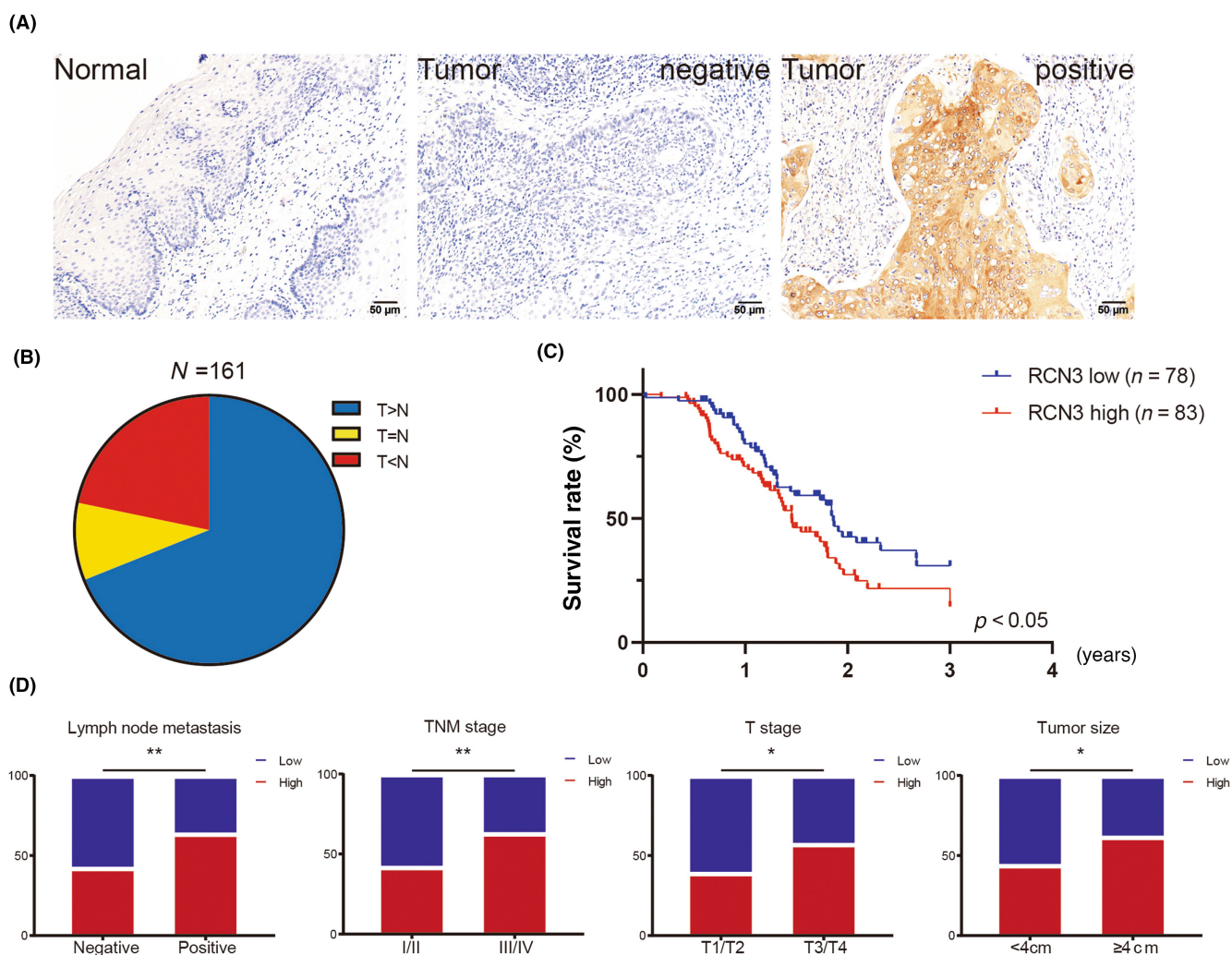


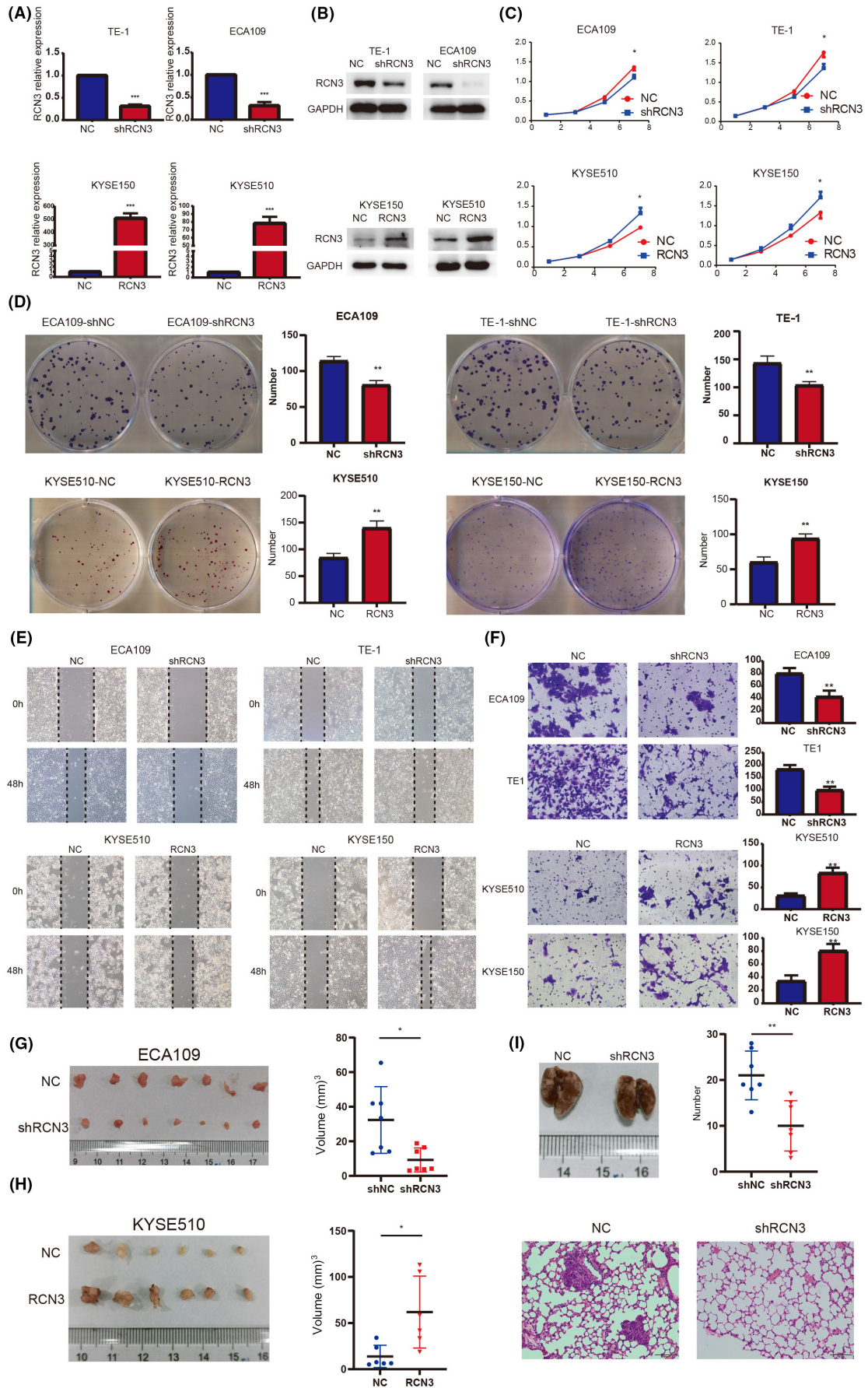
**FIGURE 1** Reticulocalbin3 (RCN3) is upregulated in esophageal squamous cell carcinoma (ESCC) and positively associated with tumor progression. (A) Immunohistochemical staining of RCN3 protein in ESCC and adjacent normal esophageal tissues. (B) Frequency of RCN3 expression categorized by Tumor [T] = Normal [N], T < N, and T > N. (C) Kaplan-Meier curve depicted the long-term survival of ESCC patients (n = 161). (D) Frequency of low/high RCN3 expression in ESCC when categorized by tumor size, lymphatic metastasis, T stage, and TNM stage. \* $p < 0.05$ , \*\* $p < 0.01$ ,  $\chi^2$

Clinical data	Number	RCN3		$\chi^2$	p value
		High	Low		
Gender					
Male	98	52	46	0.228	0.633
Female	63	31	32		
Age (years)					
>61	77	41	36	0.17	0.681
≤61	84	42	42		
Smoking					
Yes	82	45	37	0.144	0.705
No	79	38	41		
Drinking					
Yes	69	35	34	0.033	0.856
No	92	48	44		
Family history					
Yes	19	9	10	0.151	0.698
No	142	74	68		
T stage					
T1/T2	51	20	31	4.549	0.033*
T3/T4	110	63	47		
Lymph node metastasis					
Positive	69	44	25	7.214	0.007**
Negative	92	39	53		
Tumor stage					
I/II	88	37	51	7.024	0.008**
III/IV	73	46	27		
Tumor size (cm)					
<4	93	41	52	4.915	0.027*
≥4	68	42	26		
Blood vessel infiltration					
Positive	43	25	18	1.019	0.313
Negative	118	58	60		
Lymphatic vessel infiltration					
Positive	46	30	16	4.815	0.028*
Negative	115	53	62		

\* $p < 0.05$ , \*\* $p < 0.01$ .

**TABLE 1** Relationship between reticulocalbin3 (RCN3) expression and clinicopathologic features in patients with esophageal squamous cell carcinoma

**FIGURE 2** Reticulocalbin3 (RCN3) promoted cell proliferation, invasion, and metastasis. (A,B) Relative mRNA and protein expression levels of RCN3 were confirmed by quantitative RT-PCR and western blot analysis after stable RCN3 knockdown or overexpression by lentivirus in esophageal squamous cell carcinoma cells. (C) Cell proliferation capacity showed significant inhibition in interfering RCN3 groups and increase in overexpressing RCN3 groups measured by CCK-8 assays. (D) Test of proliferation ability in vitro using colony formation assay. Formation of plate colonies showed significant inhibition in interfering RCN3 groups and increase in overexpressing RCN3 groups after 2 weeks of incubation. (E) Migration ability showed significant inhibition in interfering RCN3 groups and increase in overexpressing RCN3 groups as measured by wound healing assays. (F) Invasion ability showed significant inhibition in interfering RCN3 groups and increase in overexpressing RCN3 groups as measured by Transwell invasion assays. (G) Image of nude mice tumors injected subcutaneously with RCN3 interfering ECA109 cells. Tumor volume of seven nude mice per group. (H) Image of nude mice tumors injected subcutaneously with RCN3 overexpressing KYSE510 cells. Tumor volume of six nude mice per group. (I) Image of lungs of nude mice injected with RCN3 interfering ECA109 cells through the tail vein. Number of lung metastatic nodules. \* $p < 0.05$ , \*\* $p < 0.01$ , \*\*\* $p < 0.001$ , *t*-test. NC, negative control



in the upper chamber and 500  $\mu$ l DMEM containing 15% FBS was added in the lower chamber. The cells were fixed in 4% polyformaldehyde and stained with a 0.5% crystal violet solution. Cells were observed under a light microscope; five randomly selected 200 $\times$  fields of view were counted and photographed.

## 2.8 | Apoptosis assay

Cell apoptosis was detected by the Annexin V-633 Apoptosis Detection Kit (Dojindo, AD11). Cells were collected and washed three times with PBS as instructed, followed by staining with annexin V/propidium iodide for 30 min at room temperature.

## 2.9 | Ca<sup>2+</sup> assay

Esophageal squamous cell carcinoma cells were stained with Fluo-4 AM solution for 15 min at 37°C, and detected by fluorescent microscope and flow cytometer.

## 2.10 | Transmission electron microscope assay

The ESCC cells were treated with 40  $\mu$ g/ml DDP for 24 h, collected, and fixed with 2.5% glutaraldehyde at 4°C. The ultrastructure in cells was observed using a TEM.

## 2.11 | Co-immunoprecipitation assay

The Co-IP assay was undertaken using ECA109 cell lysates and Abs for 16 h. The immune complexes were captured using Dynabeads obtained from for 1 h at room temperature under gentle rotation. The mixtures were then washed with PBST five times. Finally, the mixtures were subjected to WB analysis to test protein levels.

## 2.12 | Chromatin immunoprecipitation

ECA109/DDP cells were supplemented with 1% formaldehyde and incubated at room temperature for 10 min. The reaction was stopped by glycine and washing in cold PBS. Cells were harvested in lysis buffer and sonicated to obtain a fragment size of 300–500 bp. Immunoprecipitates were washed three times with IP Wash Buffer. Immunoprecipitated DNA was recovered in IP Elution Buffer over

4 min at 65°C, and then column-purified with QiaQuick columns. The RCN3 promoter DNA was detected using PCR amplification. Reverse transcription-PCR was carried out for samples in three groups: the IgG group (negative control), Input group (positive control), and IP group.

## 2.13 | Tail vein metastasis and nude mice xenograft experiments

We undertook a nude mouse tail vein transfer assay to observe tumor metastasis in mice *in vivo*. Four-week-old male nude mice were randomly divided into two groups and 200  $\mu$ l cell suspension was injected at a concentration of  $1 \times 10^6$  cells/ml into the tail veins. Four weeks after injection, the mice were killed, and their lungs fixed in 4% polyformaldehyde and sectioned for H&E staining.

Approximately  $1 \times 10^7$  cells were subcutaneously injected into male BALB/C nude mice. Four weeks later, those mice were killed and tumors were removed. The tumor volume (V) was calculated as:  $V = (W^2 \times L)/2$ .

All animals were managed according to the Care and Use of Medical Laboratory Animals and all experimental protocols were approved by Nanfang Hospital Animal Ethics Committee.

## 2.14 | Statistical analysis

Data are presented as the mean  $\pm$  SD. The significance of differences was analyzed by using Student's *t*-test. Correlation between the differential genes and RCN3 score were examined by Pearson's correlation coefficient. Statistical analyses were undertaken using SPSS version 23.0 for Windows. A threshold value was set at 0.05.

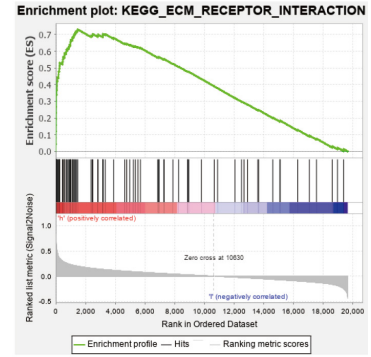
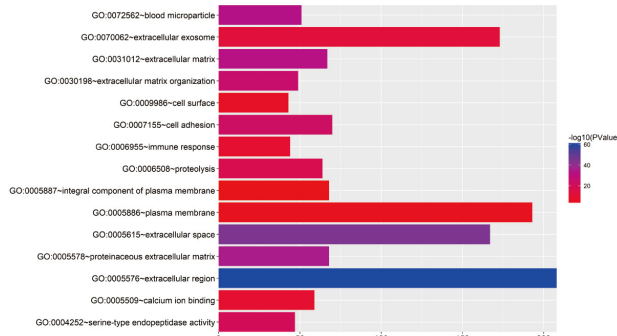
# 3 | RESULTS

## 3.1 | Reticulocalbin3 upregulated in ESCC and positively associated with tumor progression

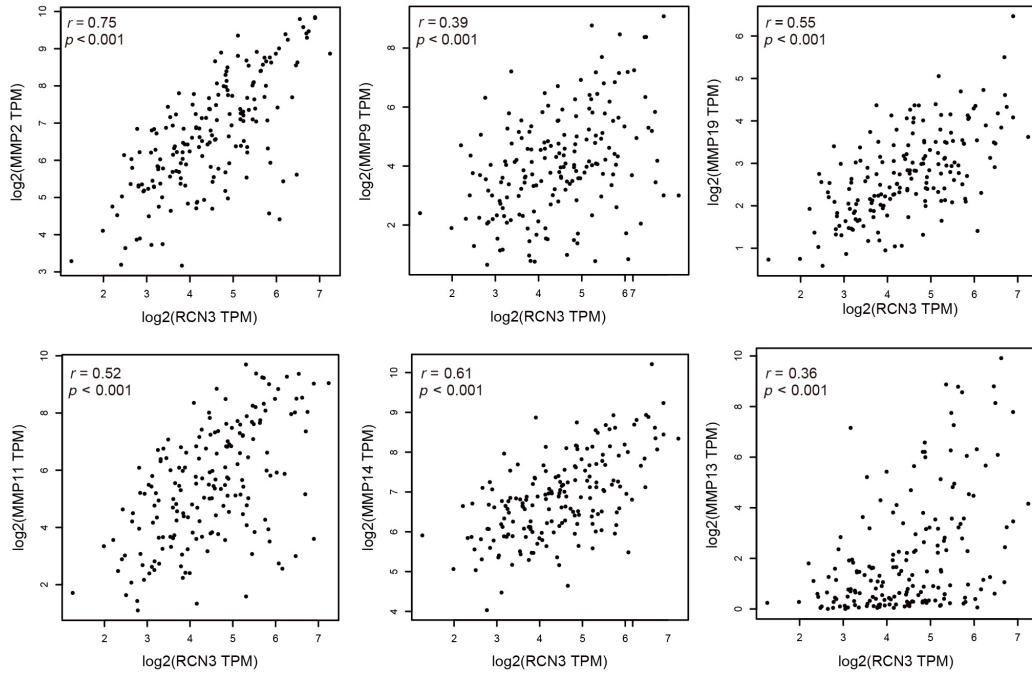
Reticulocalbin3 protein expression and its clinicopathologic significance were analyzed in surgical specimens and the paired normal tissue from 161 ESCC patients using the IHC assay (Figure 1A). We found that RCN3 was predominantly located in the cell cytoplasm. In the 161 ESCC tissue samples, the RCN3 expression in 111 cancer tissues was higher than that in paired normal tissues, the RCN3 expression in 15 cancer tissues was similar with paired normal

**FIGURE 3** Reticulocalbin3 (RCN3) regulated MMP expression. (A) Gene Ontology (GO) enrichment analysis of top 1000 RCN3 correlation genes which were classified into cellular component, molecular function, and biological process (left panel). Gene Set Enrichment Analysis for RCN3: RCN3 has positive correlation with ECM organization (right panel). (B) Bioinformatics analysis showed a positive correlation between the expression of RCN3 and MMPs in the Gene Expression Profiling Interactive Analysis database. \* $p < 0.05$ , Pearson's correlation coefficient. (C) RCN3 regulated MMP-2 and MMP-9 mRNA expression in ESCC cells. (D) RCN3 regulated MMP-2 and MMP-9 protein expression in esophageal squamous cell carcinoma cells. \* $p < 0.05$ , \*\* $p < 0.01$ , \*\*\* $p < 0.001$ , *t*-test. NC, negative control

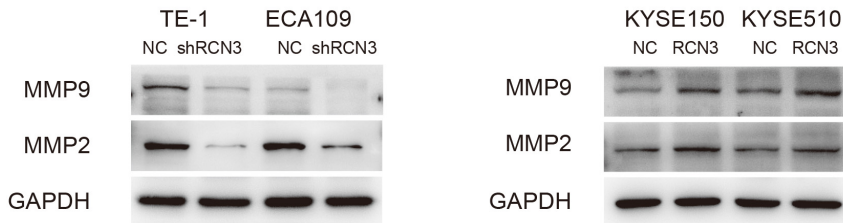
(A)



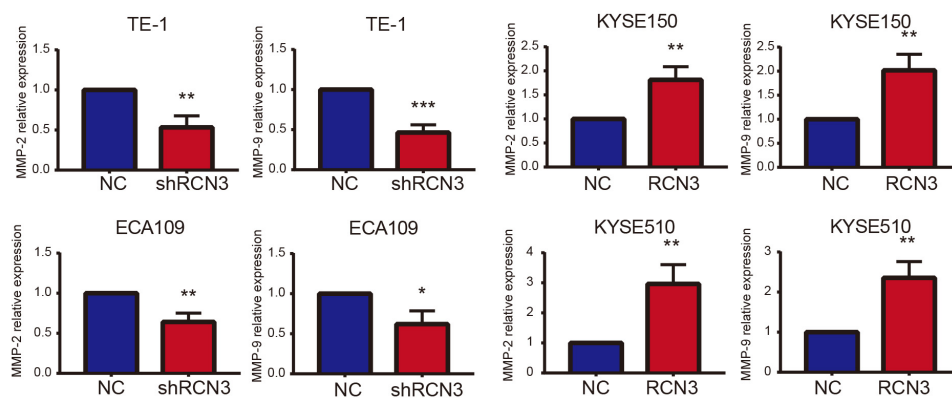
(B)



(C)



(D)



esophageal tissues, and the RCN3 expression in 35 cancer tissues was lower than that in paired normal tissues (Figure 1B). The RCN3 protein expression in ESCC tissues was significantly higher than that in paired normal tissue. The RCN3 high expression group showed poorer survival, larger tumor size, more lymph node metastasis, more lymphatic vessel infiltration, and higher T stage and TNM stage (Figure 1C,D, Table 1).

### 3.2 | Reticulocalbin3 enhanced the abilities of proliferation, migration, invasion, and metastasis of ESCC cells

Western blot and quantitative RT-PCR analyses confirmed RCN3 knockdown in TE-1 and ECA109 cells and overexpression in KYSE150 and KYSE510 cells (Figure 2A,B). Compared with the negative control (NC) group, cells in the shRCN3 group were less aggressive, with reduced proliferation, migration, and invasion, whereas the opposite effect was observed in overexpressing RCN3 (OV-RCN3) groups (Figure 2C-F). We used BALB/c nude mice as animal models. We undertook tail vein metastasis and xenograft growth assays to study whether RCN3 plays an important role in enhancing tumor metastasis and tumorigenesis in vivo. The NC group formed subcutaneous tumors with larger volume compared with the shRCN3 group, while opposite effect was observed in the OV-RCN3 groups (Figure 2G,H). The number of lung pulmonary metastases in the nude mice of the shRCN3 group was significantly decreased than the control group (Figure 2I). Together, these findings suggest that RCN3 promotes ESCC cell proliferation, invasion, and metastasis.

### 3.3 | Reticulocalbin3 promoted expression of MMPs

The Cancer Genome Atlas dataset was used to explore the genes which are correlated with RCN3 in esophageal carcinoma tissue. Gene Ontology cluster analysis and Gene Set Enrichment Analysis were performed. We found that RCN3-related genes are mainly enriched in the ECM area (Figure 3A). Furthermore, we observed that the expression of MMPs, which are located in the ECM area, are positively correlated with the expression level of RCN3 in esophageal cancer using the Gene Expression Profiling Interactive Analysis database (Figure 3B). Quantitative RT-PCR and WB assays were carried out to detect the MMP-2 and MMP-9 expression levels in ESCC cells (Figure 3C,D). Sh-RCN3 induced a significant downregulation of

MMP-2 and MMP-9. Meanwhile, OV-RCN3 induced a significant up-regulation of MMP-2 and MMP-9. The results suggested that RCN3 could induce the synergistic change of MMP-2 and MMP-9.

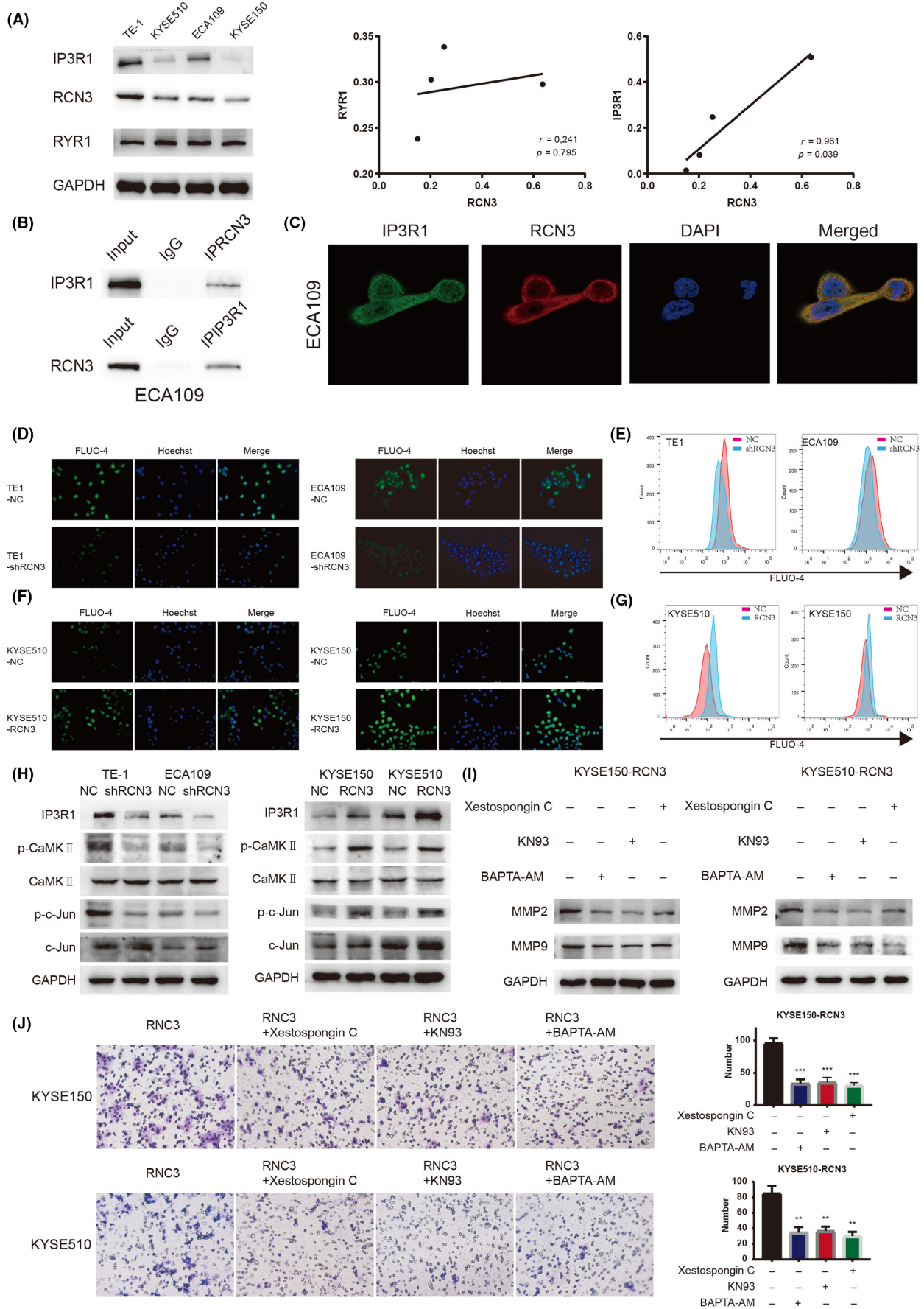
### 3.4 | Reticulocalbin3 regulated MMP-2 and MMP-9 expression through the IP3R1-Ca<sup>2+</sup>-CaMKII pathway

Reticulocalbin3 locates in the ER and is a Ca<sup>2+</sup>-binding protein containing EF-hands. Western blot analysis was used to explore the correlation between RCN3 and ER Ca<sup>2+</sup> channel protein in ESCC cells. We found that RCN3 expression showed a significant positive correlation with IP3R1 but not RYR1 (Figure 4A). Next, we undertook Co-IP and immunofluorescence analyses to investigate the interaction between RCN3 and IP3R1 in ECA109 cells. The Co-IP analysis revealed protein-protein interaction between RCN3 and IP3R1, indicating that endogenous human RCN3 was physically associated with IP3R1 (Figure 4B). Furthermore, immunofluorescence localization showed that RCN3 and IP3R1 were coexpressed in cytoplasm, by confocal microscopy (Figure 4C). Results showed that there was an interaction between RCN3 and IP3R1. Furthermore, we observed increased IP3R1 expression in OV-RCN3 cells, whereas the opposite effect was observed in shRCN3 cells (Figure 4H). It indicated that RCN3 regulated the protein level of IP3R1. We also found that the intracellular Ca<sup>2+</sup> level also changed. The intracellular Ca<sup>2+</sup> level was reduced in shRCN3 cells (Figure 4D,E), whereas the opposite effect was found in OV-RCN3 cells (Figure 4F,G). We also detected the change of Ca<sup>2+</sup> signaling in ESCC cell lines. Downregulation of RCN3 caused significantly decreased phosphorylation levels of CaMKII and c-Jun compared with the control group (Figure 4H). In contrast, overexpression of RCN3 led to sustained phosphorylation of CaMKII and c-Jun (Figure 4H). The expression of MMP-2 and MMP-9 were inhibited by Ca<sup>2+</sup> chelator (BAPTA AM), CaMKII inhibitor (KN93), or IP3R inhibitor (Xestospongine C) in OV-RCN3 ESCC cells (Figure 4I). The Ca<sup>2+</sup> chelator and IP3R/CaMKII inhibitors inhibited the invasion abilities of OV-RCN3 cells (Figure 4J). The above results indicated that RCN3 promotes the expression of MMP-2 and MMP-9 by regulating the IP3R1-Ca<sup>2+</sup>-CaMKII-c-Jun signaling pathway.

### 3.5 | Knockdown of RCN3 repressed DDP resistance of ESCC cells

Cisplatin resistance of ESCC (ESCC/DDP) cells was prepared in vitro by intermittently exposing ESCC cells to increasing concentrations

**FIGURE 4** Reticulocalbin3 (RCN3) regulated MMP-2 and MMP-9 expression through inositol 1,4,5-trisphosphate receptor 1 (IP3R1)-Ca<sup>2+</sup>-calcium/calmodulin-dependent protein kinase (CaMKII). (A) In esophageal squamous cell carcinoma (ESCC) cell lines, RCN3 is positively correlated with IP3R1 expression. \**p* < 0.05, Pearson's correlation coefficient. (B) Co-IP analysis showed that RCN3 interacted with IP3R1. (C) Immunofluorescence staining showed the expression and localization of RCN3 and IP3R1 in ECA109 cells. (D-G) Fluo-4 AM showed intracellular Ca<sup>2+</sup> concentration. (H) Western blot analysis the expression of related proteins of the IP3R1-Ca<sup>2+</sup>-CaMKII-c-Jun signaling pathway. (I) Expression of MMP-2 and MMP-9 inhibited by IP3R-Ca<sup>2+</sup>-CaMKII blockers in OV-RCN3 ESCC cells. (J) Invasion ability of OV-RCN3 ESCC cell inhibited by IP3R-Ca<sup>2+</sup>-CaMKII blockers. \**p* < 0.05, \*\**p* < 0.01, \*\*\**p* < 0.001, *t*-test. NC, negative control



of DDP for 6 months. We detected the expression of resistance markers in ESCC cell lines. The results showed that the expression levels of MDR1 and ABCG2 in the ESCC/DDP cells were up-regulated as compared to the control cells (Figure 5A). Cell survival rate was determined by CCK-8 assays. The  $IC_{50}$  DDP values of the ECA109 and ECA109/DDP cells were 33.31 and 156.35  $\mu\text{g/ml}$ , respectively, and the KYSE150 and KYSE150/DDP cells were 205.4 and 760.69  $\mu\text{g/ml}$ , respectively (Figure 5B). The resistance indexes were 4.69 and 3.7. The results suggested that DDP resistance of ESCC cells were successfully established. The expression of RCN3 protein in ESCC/DDP cells was significantly higher than in normal ESCC cells (Figure 5A). CCK-8 assays were performed to detect the cell survival rate. Compared with the control group, knockdown of RCN3 decreased the survival rate induced by DDP (Figure 5C). After DDP treatment, ESCC/DDP cells showed less ER and mitochondria swelling compared with normal ESCC cells. Sh-RCN3 could promote ER and mitochondria swelling (Figure 5D). These findings suggest that downregulation of RCN3 enhances chemosensitivity induced by DDP in ESCC cells.

### 3.6 | Reticulocalbin3 promoted chemoresistance by targeting IP3R1/ $\text{Ca}^{2+}$ through inhibiting ROS production

Flow cytometry assay was used to detect the apoptosis rate, mitochondrial membrane potential, and ROS level. Compared with the control group, knockdown of RCN3 increased the apoptosis rate and decreased mitochondrial membrane potential induced by DDP (Figure 5E,F). Meanwhile, ROS levels were significantly upregulated in shRCN3 ESCC/DDP cells (Figure 5G). All the above phenomena could be reversed by  $\text{Ca}^{2+}$  chelator (BAPTA AM) in shRCN3 ESCC/DDP cells (Figure 5E-G). In contrast, compared with the control group, overexpression of RCN3 decreased apoptosis rates and increased mitochondrial membrane potential induced by DDP (Figure 5H,I). The ROS levels were also significantly downregulated in OV-RCN3 ESCC cells (Figure 5J). Knockdown of IP3R1 increased apoptosis rates and ROS levels while decreasing mitochondrial membrane potential (Figure 5H-J) in both the control group and OV-RCN3 group. Finally, RCN3 protein expression and its chemoresistance were

analyzed in 35 patients who had received platinum-based neoadjuvant chemotherapy before surgery. Chemotherapy reactivity was defined by TRG (0-3). Expression of RCN3 protein in resistant ESCC pretreatment biopsy tissues (postoperative tissues, TRG2/3) was significantly higher than in chemotherapy-sensitive pretreatment tissues (postoperative tissues, TRG0/1) (Figure 5K). Taken together, the results indicate that RCN3 expression is positively associated with chemoresistance in ESCC. In summary, these data demonstrate that overexpression of RCN3 promotes chemoresistance by targeting IP3R1/ $\text{Ca}^{2+}$  through inhibiting ROS production.

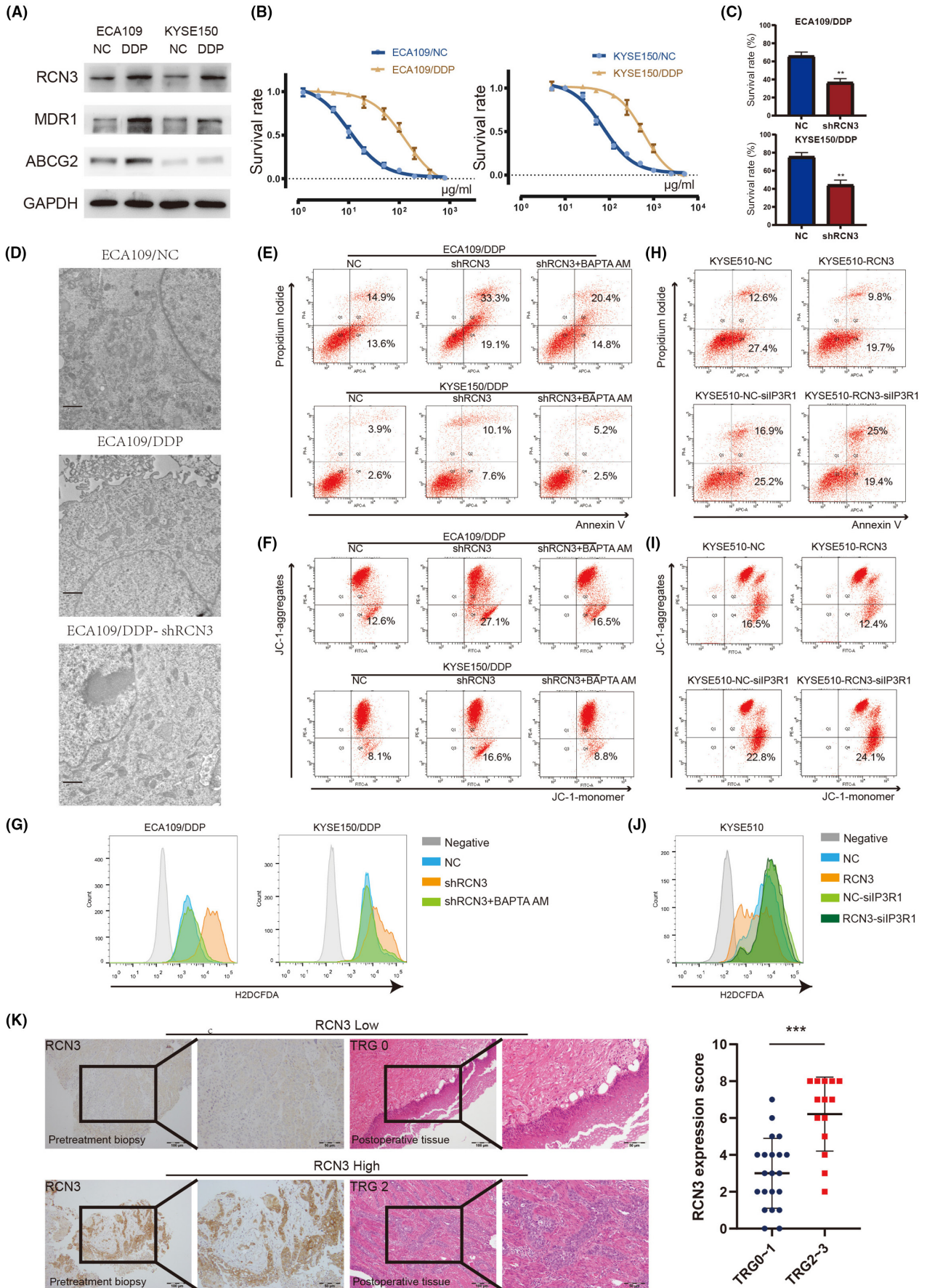
### 3.7 | Reticulocalbin3 expression in ESCC/DDP cells regulated by HIF-1 $\alpha$

Reticulocalbin3 expression was statistically correlated with HIF-1 $\alpha$  in The Cancer Genome Atlas (Figure 6A). We detected the expression of RCN3 and HIF-1 $\alpha$  in 65 cases of ESCC tissues by IHC. We found that there was also a positive relationship between the expression of RCN3 and HIF-1 $\alpha$  ( $p = 0.029$ ,  $\chi^2$ -test) (Figure 6B, Table 2). The expression of HIF-1 $\alpha$  protein in ESCC/DDP cells was significantly higher than in normal ESCC cells (Figure 6C). We undertook a ChIP experiment to clarify whether HIF-1 $\alpha$  has a regulatory effect on RCN3 expression. The results showed that HIF-1 $\alpha$  could bind with promoter regions of RCN3 in ECA109/DDP cells (Figure 6D). Indeed, RCN3 expression was abolished by silencing HIF-1 $\alpha$  (Figure 6E). Thus, these results suggest that HIF-1 $\alpha$  could directly induce RCN3 expression through binding to the promoter region. Knockdown of RCN3 or HIF-1 $\alpha$  inhibited the survival rate of ESCC/DDP cells, which could all be reversed by BAPTA AM (Figure 6F). Thus, HIF-1 $\alpha$  induces DDP resistance by regulating the expression of RCN3.

## 4 | DISCUSSION

Upregulated expression of RCN3 protein in ESCC tissue was identified by TMT in our recent research.<sup>21</sup> So far there has been no study on how RCN3 regulates tumor progression. Expression levels of RCN3 are ambiguous in different cancers.<sup>17-20</sup> Our data indicated that RCN3 was upregulated in ESCC tissues. Therefore, the function

**FIGURE 5** Reticulocalbin3 (RCN3) promoted chemoresistance by targeting inositol 1,4,5-trisphosphate receptor 1 (IP3R1)/ $\text{Ca}^{2+}$  through inhibiting reactive oxygen species (ROS) production. (A) Western blot showed the expression of chemoresistance proteins MDR1(D-11), ABCG2, and RCN3. (B) After treatment with different concentrations of cisplatin (DDP), CCK-8 showed the cell growth inhibition rate. (C) CCK-8 showed the survival rate of drug-resistant cells after interfering RCN3 expression. (D) Transmission electron microscopy showed the structure of ECA109, ECA109/DDP, and ECA109/DDP-shRCN3 cells. (E) Apoptosis analysis showed apoptosis rates of interfering RCN3  $\pm$  calcium chelator (BAPTA AM) resistant cell line, treated with DDP 24 h. (F) Quantitative analysis of mitochondrial membrane potential measurements with JC-1. The change of interfering RCN3  $\pm$  calcium chelator (BAPTA AM) resistant cell line, treated with DDP 24 h. (G) ROS analysis showed reactive oxygen of interfering RCN3  $\pm$  calcium chelator (BAPTA AM) resistant cell line, treated with DDP 24 h. (H) Apoptosis analysis showed apoptosis rate of overexpression of RCN3  $\pm$  siIP3R1, treated with DDP for 24 h. (I) Quantitative analysis of mitochondrial membrane potential measurements with JC-1. The change of overexpression of RCN3  $\pm$  siIP3R1 resistant cell line, treated with DDP 24 h. (J) ROS analysis showed overexpression of RCN3  $\pm$  si-IP3R1, treated with DDP 24 h. (K) Immunohistochemical staining of RCN3 protein in esophageal squamous cell carcinoma (ESCC) biopsy tissues (left panel). H&E staining of platinum-based chemotherapy ESCC tissues (right panel). \* $p < 0.05$ , \*\* $p < 0.01$ , \*\*\* $p < 0.001$ , t-test. NC, negative control



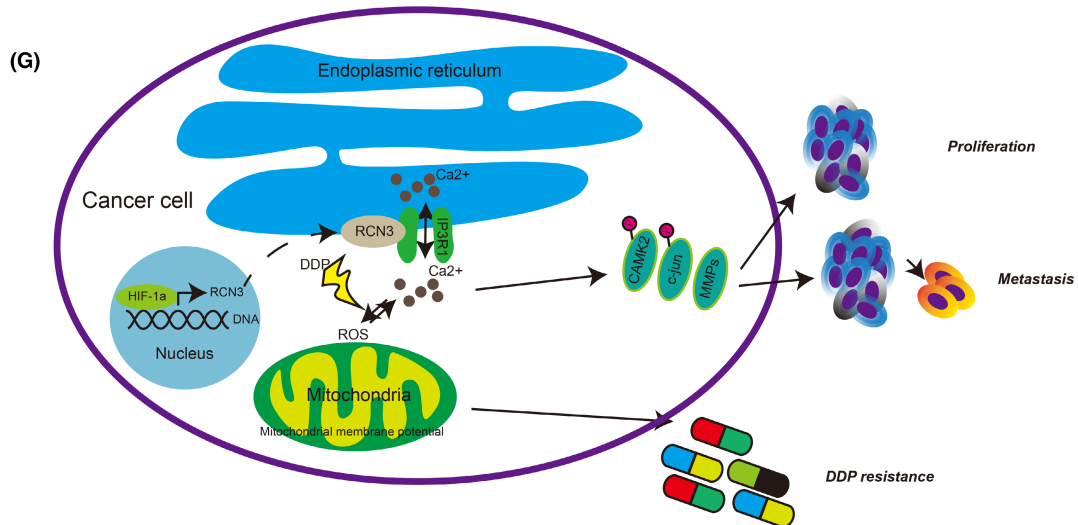
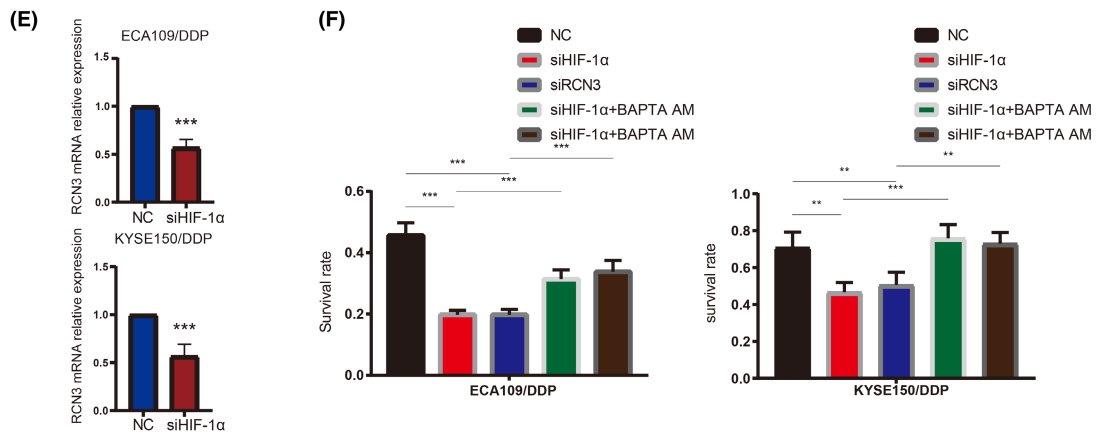
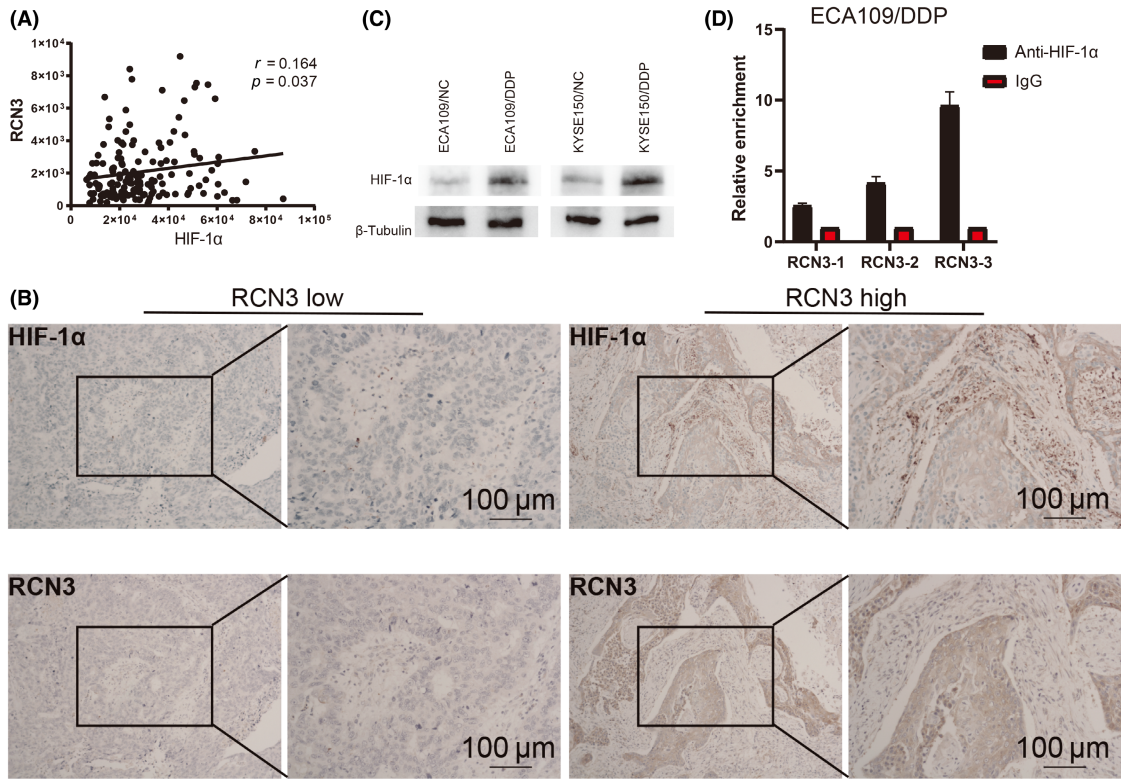


**FIGURE 6** Reticulocalbin3 (RCN3) expression is regulated by hypoxia inducible factor-1 $\alpha$  (HIF-1 $\alpha$ ) in esophageal squamous cell carcinoma (ESCC)/cisplatin (DDP) cells. (A) The Cancer Genome Atlas database analysis found that the transcription factor HIF-1 $\alpha$  was significantly positively correlated with RCN3. \* $p < 0.05$ , Pearson's correlation coefficient. (B) Immunohistochemistry showed that RCN3 and HIF-1 $\alpha$  in ESCC tissues. (C) Western blot analysis of HIF-1 $\alpha$  protein expression in sensitive cell lines and chemoresistant cell lines. (D) ChIP experiments showed that HIF-1 $\alpha$  could bind to the RCN3 promoter region. (E) Quantitative RT-PCR analysis showed that silence of HIF-1 $\alpha$  could inhibit RCN3 expression. (F) CCK-8 assays analysis showed that silence of HIF-1 $\alpha$  or RCN3,  $\pm$  calcium ion chelator (BAPTA AM), changes in cell survival rate with DDP treatment 24 h. (G) Schematic showing that RCN3 regulates Ca<sup>2+</sup> homeostasis to promote ESCC progression. \* $p < 0.05$ , \*\* $p < 0.01$ , \*\*\* $p < 0.001$ , t-test. NC, negative control

**TABLE 2** Correlation of expression levels of reticulocalbin3 (RCN3) and hypoxia inducible factor-1 $\alpha$  (HIF-1 $\alpha$ ) in esophageal squamous cell carcinoma

	RCN3		$\chi^2$	p value
	High	Low		
HIF-1 $\alpha$				
High	22	9	4.767	0.029
Low	15	19		

of RCN3 in carcinogenesis is probably associated with tissue-specific molecular profiles. RCN3 could serve as an oncogene during ESCC progression, enhancing tumor growth and facilitating lymphatic metastasis in ESCC patients. Therefore, RCN3 could be used to predict ESCC patients' prognosis.

In the present study, we investigated the role of RCN3 in ESCC by conducting gain and loss of function analyses. Overexpression of RCN3 in ESCC cells promoted proliferation, migration, and invasion properties in vitro as well as driving tumor growth and facilitating metastasis in vivo, suggesting that RCN3 might promote ESCC progression.

In our study, we found that RCN3 had a significant positive correlation with ECM in esophageal carcinoma. The role of ECM in tumor progression is getting more and more attention.<sup>22</sup> In the dynamic balance of ECM, small changes can have a significant impact on tumor cell proliferation, migration, invasion, and apoptosis.<sup>23</sup> We found that multiple MMPs enriched in the ECM were related to RCN3 expression. Matrix metalloproteinases participate in several physiological processes, such as inflammation, angiogenesis, immune and wound healing, as well as tumor progression.<sup>24,25</sup> Both MMP-2 and MMP-9 belong to the gelatinases. They promote tumor invasion, matrix adhesion, and metastasis.<sup>26,27</sup> In our present study, we certified that RCN3 enhanced the expression of MMP-2 and MMP-9 in ESCC cells, so that RCN3 could regulate MMP-induced progression of ESCC.

Reticulocalbin3 contains EF-hands and is mainly located in the ER. It has been reported that EF-hands play an important role in calcium buffering in the cytosol.<sup>28</sup> As the ER is the largest Ca<sup>2+</sup> reservoir in the cell, it suggests that RCN3 might participate in the regulation of intracellular Ca<sup>2+</sup> homeostasis. Two important calcium channels in the ER are RYRs and IP3Rs.<sup>29</sup> In our study, RCN3 showed a significant positive correlation with IP3R1 but not RYR1 in ESCC cells. We also reported that RCN3 protein was colocalized and interacted with IP3R1. In OV-RCN3 ESCC cells, the expression of IP3R1 was significantly upregulated, accompanied by an increase in intracellular

Ca<sup>2+</sup>. The above findings are consistent with the research of IP3R1 in prostate cancer, which also illustrates a positive relationship between high IP3R1 expression and malignant phenotype.<sup>30</sup> In another study, the opening of IP3R channels increases intracellular Ca<sup>2+</sup> levels and induces cell apoptosis.<sup>31</sup> We speculate that IP3R1 regulates intracellular Ca<sup>2+</sup> and affects tumor progression in different tumor microenvironments. Ca<sup>2+</sup> promotes tumor progression normally, but it induces cell apoptosis when there is Ca<sup>2+</sup> overloaded.

As an important second messenger in cells, Ca<sup>2+</sup> activated protein kinases induce protein phosphorylation and promote downstream protein transcription activation. Here, we detected increased activities of CaMKII-c-Jun signaling pathways in OV-RCN3 ESCC cells. The activation of the CaMKII-c-Jun pathways is required for expression of MMP-2 and MMP-9. Both MMP-2 and MMP-9 increase tumor cell migration ability and induce vascular remodeling after CaMKII-c-Jun activation.<sup>32,33</sup> Furthermore, the expression of MMP-2 and MMP-9 was inhibited by Ca<sup>2+</sup> chelator, IP3R antagonist, or CaMKII inhibitor in OV-RCN3 ESCC cells. In conclusion, we speculate that RCN3 promotes the aggressive properties of ESCC cells through activating the IP3R1-Ca<sup>2+</sup>-CaMKII-MMP signaling pathway.

Cisplatin is the first-line chemotherapeutic drug for esophageal cancer, and Ca<sup>2+</sup> tolerance is one of the important reasons for DDP resistance.<sup>34</sup> Our previous study has shown that RCN3 can regulate intracellular Ca<sup>2+</sup> homeostasis by targeting IP3R1. In order to explore the role of RCN3 in DDP resistance, we prepared DDP-resistant ESCC cells through stepwise exposure to increasing DDP concentrations for 6 months. Upregulation of IC<sub>50</sub> and resistance proteins such as MDR1(D-11) and ABCG2<sup>35</sup> indicated that the cells acquired chemoresistance. Meanwhile, RCN3 was upregulated in ESCC/DDP cells. We also found that RCN3 showed a significant correlation with chemoresistance and was overexpressed in pretreatment biopsies of chemoresistance patients. Therefore, RCN3 could be used to predict ESCC patients' chemosensitivity.

Chemotherapy is believed to directly or indirectly result in induction of apoptosis.<sup>36</sup> Decreased mitochondrial transmembrane potential of the cell is one of the characteristics of early apoptosis.<sup>37</sup> In this study, we observed that knockdown of RCN3 promoted DDP-induced apoptosis, and decreased mitochondrial transmembrane potential of ESCC cells, along with the alterations of microstructure, such as increased ER and mitochondria swelling. We also showed that silencing RCN3 promoted DDP-induced apoptosis and ROS, which can be reversed by Ca<sup>2+</sup> chelator. Inhibition of IP3R1 expression promoted DDP-induced apoptosis and ROS either in normal

or overexpressing RCN3 ESCC cells. The interaction between  $\text{Ca}^{2+}$  overload and ROS production is correlated with cell apoptosis.<sup>38</sup> Our work showed that low expression of RCN3 can increase DDP-induced apoptosis of ESCC cells by targeting IP3R1- $\text{Ca}^{2+}$ . Therefore, RCN3 can be used as a potential target for clinical treatment of DDP-resistant esophageal cancer.

Hypoxia inducible factor-1 $\alpha$  has been proven to be an essential transcription factor in chemoresistance development. Hypoxia inducible factor-1 $\alpha$  regulates the intracellular  $\text{Ca}^{2+}$  concentration and participates in carboplatin resistance.<sup>39</sup> In our study, HIF-1 $\alpha$  was upregulated in ESCC/DDP cells, which is consistent with previous studies in NSCLC and ovarian cancer.<sup>40,41</sup> We showed that HIF-1 $\alpha$  upregulated RCN3 expression through binding to RCN3 promoter. Inhibition of HIF-1 $\alpha$  promoted DDP-induced apoptosis, which can be reversed by BAPTA AM. This effect is consistent with RCN3. It showed that the accumulation of HIF-1 $\alpha$  induced chemotherapy resistance through increasing RCN3 transcription.

In conclusion, our findings supported the oncogenic function of RCN3 in ESCC. Overexpression of RCN3 was positively associated with T stage, lymphatic metastasis, lymphatic vessel infiltration, TNM stage, and chemoresistance in ESCC. Reticulocalbin3 functions as  $\text{Ca}^{2+}$  regulator. Overexpression of RCN3 increased ESCC cells' malignant phenotype by targeting IP3R1- $\text{Ca}^{2+}$ -CaMKII-MMP signaling. Furthermore, RCN3 is involved in  $\text{Ca}^{2+}$  tolerance, which induced DDP resistance (Figure 6G). In general, our study suggested that RCN3 could be a molecular biomarker of ESCC progression and inhibition of RCN3 could supply a potential therapy for ESCC.

#### AUTHOR CONTRIBUTIONS

RC and PW contributed equally to this work. JL contributed to study design, obtaining funding, and study supervision. RC and PW performed the experiments and wrote the manuscript. XZ, XSL, and RXD contributed to the collection of patient samples and interpreted the results. XYW and CH contributed data and statistical analysis. All authors approved the final manuscript.

#### ACKNOWLEDGMENTS

This work was supported by the National Natural Science Foundation of China (82173298, 81672441), the Natural Science Foundation of Guangdong Province, China (2016A030313580, 2017A030313607, and 2022A1515012390), and Guangzhou Science and Technology Project (202102080076).

#### DISCLOSURE

The authors have no conflict of interest.

#### ETHICS STATEMENT

This study was approved by the Medical Ethical Committee of Nanfang Hospital. Written informed consent was received from all patients.

Registry and registration no. of the study/trial: N/A.

Animal studies: All animals were managed according to the Care and Use of Medical Laboratory Animals and all experimental protocols were approved by Nanfang Hospital Animal Ethics Committee.

#### ORCID

Jie Lin  <https://orcid.org/0000-0002-5952-2319>

#### REFERENCES

1. Siegel RL, Miller KD, Fuchs HE, Jemal A. Cancer Statistics, 2021. *CA Cancer J Clin*. 2021;71(1):7-33.
2. Chen W, Zheng R, Baade PD, et al. Cancer statistics in China, 2015. *CA Cancer J Clin*. 2016;66(2):115-132.
3. Pennathur A, Gibson MK, Jobe BA, Luketich JD. Oesophageal carcinoma. *Lancet*. 2013;381(9864):400-412.
4. Merkow RP, Bilimoria KY, Keswani RN, et al. Treatment trends, risk of lymph node metastasis, and outcomes for localized esophageal cancer. *J Natl Cancer Inst*. 2014;106(7):dju133.
5. Mao C, Zeng X, Zhang C, et al. Mechanisms of pharmaceutical therapy and drug resistance in esophageal cancer. *Front Cell Dev Biol*. 2021;9:612451.
6. Honore B. The rapidly expanding CREC protein family: Members, localization, function, and role in disease. *Bioessays*. 2009;31(3):262-277.
7. Ding D, Huang H, Jiang W, et al. Reticulocalbin-2 enhances hepatocellular carcinoma proliferation via modulating the EGFR-ERK pathway. *Oncogene*. 2017;36(48):6691-6700.
8. Chen X, Shao W, Huang H, Feng X, Yao S, Ke H. Overexpression of RCN1 correlates with poor prognosis and progression in non-small cell lung cancer. *Hum Pathol*. 2019;83:140-148.
9. Uzoie AC, Selevsek N, Wahlander A, et al. Targeted proteomics for multiplexed verification of markers of colorectal tumorigenesis. *Mol Cell Proteomics*. 2017;16(3):407-427.
10. Gomez J, Areeb Z, Stuart SF, et al. EGFRvIII promotes cell survival during endoplasmic reticulum stress through a reticulocalbin 1-Dependent mechanism. *Cancers (Basel)*. 2021;13(6):1198.
11. Giribaldi G, Barbero G, Mandili G, et al. Proteomic identification of Reticulocalbin 1 as potential tumor marker in renal cell carcinoma. *J Proteomics*. 2013;91:385-392.
12. Liu X, Zhang N, Wang D, et al. Downregulation of reticulocalbin-1 differentially facilitates apoptosis and necroptosis in human prostate cancer cells. *Cancer Sci*. 2018;109(4):1147-1157.
13. Xu M, Che L, Yang Z, et al. Proteomic analysis of fetal ovaries reveals that primordial follicle formation and transition are differentially regulated. *Biomed Res Int*. 2017;2017:6972030-6972011.
14. Jin J, Li Y, Ren J, et al. Neonatal respiratory failure with retarded perinatal lung maturation in mice caused by reticulocalbin 3 disruption. *Am J Respir Cell Mol Biol*. 2016;54(3):410-423.
15. Jin J, Shi X, Li Y, et al. Reticulocalbin 3 Deficiency in Alveolar Epithelium Exacerbated Bleomycin-induced Pulmonary Fibrosis. *Am J Respir Cell Mol Biol*. 2018;59(3):320-333.
16. Park NR, Shetye SS, Bogush I, et al. Reticulocalbin 3 is involved in postnatal tendon development by regulating collagen fibrillogenesis and cellular maturation. *Sci Rep*. 2021;11(1):10868.
17. Hagedorn M, Siegfried G, Hooks KB, Khatib AM. Integration of zebrafish fin regeneration genes with expression data of human tumors in silico uncovers potential novel melanoma markers. *Oncotarget*. 2016;7(44):71567-71579.
18. Zhou Y, Bian S, Zhou X, et al. Single-Cell multiomics sequencing reveals prevalent genomic alterations in tumor stromal cells of human colorectal cancer. *Cancer Cell*. 2020;38(6):818-828.e5.
19. Li Y, Liang Q, Wen YQ, et al. Comparative proteomics analysis of human osteosarcomas and benign tumor of bone. *Cancer Genet Cytogenet*. 2010;198(2):97-106.
20. Hou Y, Li Y, Gong F, et al. A preliminary study on RCN3 protein expression in non-small cell lung cancer. *Clin Lab*. 2016;62(3):293-300.
21. Cai R, Wang P, Zhao X, et al. LTBP1 promotes esophageal squamous cell carcinoma progression through epithelial-mesenchymal

- transition and cancer-associated fibroblasts transformation. *J Transl Med*. 2020;18(1):139.
22. Rauner G, Kuperwasser C. Microenvironmental control of cell fate decisions in mammary gland development and cancer. *Dev Cell*. 2021;56(13):1875-1883.
  23. Bonnans C, Chou J, Werb Z. Remodelling the extracellular matrix in development and disease. *Nat Rev Mol Cell Biol*. 2014;15(12):786-801.
  24. Cox TR. The matrix in cancer. *Nat Rev Cancer*. 2021;21(4):217-238.
  25. Alaseem A, Alhazzani K, Dondapati P, Alobid S, Bishayee A, Rathinavelu A. Matrix Metalloproteinases: A challenging paradigm of cancer management. *Semin Cancer Biol*. 2019;56:100-115.
  26. Klein G, Vellenga E, Fraaije MW, Kamps WA, de Bont ES. The possible role of matrix metalloproteinase (MMP)-2 and MMP-9 in cancer, e.g. Acute leukemia. *Crit Rev Oncol Hematol*. 2004;50(2):87-100.
  27. Jacob A, Prekeris R. The regulation of MMP targeting to invadopodia during cancer metastasis. *Front Cell Dev Biol*. 2015;3:4.
  28. Elies J, Yanez M, Pereira T, Gil-Longo J, Macdougall DA, Campos-Toimil M. An update to calcium binding proteins. *Adv Exp Med Biol*. 2020;1131:183-213.
  29. Toprak U, Dogan C, Hegedus D. A Comparative Perspective on Functionally-Related, Intracellular Calcium Channels: The Insect Ryanodine and Inositol 1,4,5-Trisphosphate Receptors. *Biomolecules*. 2021;11(7):1031.
  30. Boutin B, Tajeddine N, Monaco G, et al. Endoplasmic reticulum Ca(2+) content decrease by PKA-dependent hyperphosphorylation of type 1 IP3 receptor contributes to prostate cancer cell resistance to androgen deprivation. *Cell Calcium*. 2015;57(4):312-320.
  31. Xu X, Chen D, Ye B, Zhong F, Chen G. Curcumin induces the apoptosis of non-small cell lung cancer cells through a calcium signaling pathway. *Int J Mol Med*. 2015;35(6):1610-1616.
  32. Chen YS, Lu MJ, Huang HS, Ma MC. Mechanosensitive transient receptor potential vanilloid type 1 channels contribute to vascular remodeling of rat fistula veins. *J Vasc Surg*. 2010;52(5):1310-1320.
  33. Dai L, Zhuang L, Zhang B, et al. DAG/PKCdelta and IP3/Ca(2+)/CaMK IIbeta operate in parallel to each other in PLCgamma1-Driven cell proliferation and migration of human gastric adenocarcinoma cells, through Akt/mTOR/S6 pathway. *Int J Mol Sci*. 2015;16(12):28510-28522.
  34. Xue Y, Morris JL, Yang K, et al. SMARCA4/2 loss inhibits chemotherapy-induced apoptosis by restricting IP3R3-mediated Ca(2+) flux to mitochondria. *Nat Commun*. 2021;12(1):5404.
  35. Robey RW, Pluchino KM, Hall MD, Fojo AT, Bates SE, Gottesman MM. Revisiting the role of ABC transporters in multidrug-resistant cancer. *Nat Rev Cancer*. 2018;18(7):452-464.
  36. Burke PJ. Mitochondria, bioenergetics and apoptosis in cancer. *Trends Cancer*. 2017;3(12):857-870.
  37. Bock FJ, Tait S. Mitochondria as multifaceted regulators of cell death. *Nat Rev Mol Cell Biol*. 2020;21(2):85-100.
  38. Joseph SK, Booth DM, Young MP, Hajnoczky G. Redox regulation of ER and mitochondrial Ca(2+) signaling in cell survival and death. *Cell Calcium*. 2019;79:89-97.
  39. Lu H, Chen I, Shimoda LA, et al. Chemotherapy-Induced Ca(2+) Release Stimulates Breast Cancer Stem Cell Enrichment. *Cell Rep*. 2017;18(8):1946-1957.
  40. Zhang F, Duan S, Tsai Y, et al. Cisplatin treatment increases stemness through upregulation of hypoxia-inducible factors by interleukin-6 in non-small cell lung cancer. *Cancer Sci*. 2016;107(6):746-754.
  41. Wang WJ, Sui H, Qi C, et al. Ursolic acid inhibits proliferation and reverses drug resistance of ovarian cancer stem cells by downregulating ABCG2 through suppressing the expression of hypoxia-inducible factor-1alpha in vitro. *Oncol Rep*. 2016;36(1):428-440.

#### SUPPORTING INFORMATION

Additional supporting information can be found online in the Supporting Information section at the end of this article.

**How to cite this article:** Cai R, Wang P, Zhao X, et al. Reticulocalbin3: A Ca<sup>2+</sup> homeostasis regulator that promotes esophageal squamous cell carcinoma progression and cisplatin resistance. *Cancer Sci*. 2022;113:3593-3607. doi: [10.1111/cas.15487](https://doi.org/10.1111/cas.15487)